

On the Convergence of Jacobian-Free Backpropagation for Optimal Control Problems with Implicit Hamiltonians

Eric Gelphman¹ Deepanshu Verma² Nicole Tianjiao Yang³ Stanley Osher⁴ Samy Wu Fung¹

Abstract

Optimal feedback control with implicit Hamiltonians poses a fundamental challenge for learning-based value function methods due to the absence of closed-form optimal control laws. Recent work (Gelphman et al., 2025) introduced an implicit deep learning approach using Jacobian-Free Backpropagation (JFB) to address this setting, but only established sample-wise descent guarantees. In this paper, we establish convergence guarantees for JFB in the stochastic minibatch setting, showing that the resulting updates converge to stationary points of the expected optimal control objective. We further demonstrate scalability on substantially higher-dimensional problems, including multi-agent optimal consumption and swarm-based quadrotor and bicycle control. Together, our results provide both theoretical justification and empirical evidence for using JFB in high-dimensional optimal control with implicit Hamiltonians.

1. Introduction

We aim to generate semi-global feedback controllers for high-dimensional control problems of the form

$$\min_{u \in U} \int_0^T L(s, z_x, u) ds + G(z_x(T)), \quad (1)$$

$$\text{subject to } \dot{z}_x = f(t, z_x, u), \quad z_x(0) = x,$$

where $z_x \in \mathbb{R}^n$ is the state trajectory with dynamics f and initial condition x , $u(t) \in U \subset \mathbb{R}^m$ is the control input, L is the running cost, and G is the terminal cost. The subscript in z_x denotes the dependence of the state on the initial condition x .

¹Department of Applied Mathematics and Statistics, Colorado School of Mines ²Department of Mathematical Sciences, Clemson University ³Department of Mathematics, University of Tennessee Knoxville ⁴Department of Mathematics, University of California Los Angeles. Correspondence to: Samy Wu Fung <swufung@mines.edu>.

Preprint. February 3, 2026.

The Pontryagin Maximum Principle (PMP) (Pontryagin, 2018; Kopp, 1962) provides a first-order characterization of optimal solutions to continuous-time control problems by introducing an adjoint (costate) variable that couples the system dynamics and the objective. In particular, PMP associates to the control problem a generalized Hamiltonian of the form

$$\mathcal{H}(t, z_x, p_x, u) = -\langle p_x, f(t, z_x, u) \rangle - L(t, z_x, u), \quad (2)$$

where the adjoint variable p_x evolves backward in time and encodes the sensitivity of the optimal cost with respect to the state. An optimal control u^* must satisfy a two-point boundary value problem consisting of the state dynamics and adjoint dynamics,

$$\dot{z}_x(t) = -\nabla_p \mathcal{H}(t, z_x(t), p_x(t), u^*(t)),, \quad (3)$$

$$\dot{p}_x(t) = \nabla_z \mathcal{H}(t, z_x(t), p_x(t), u^*(t)), \quad (4)$$

with $z_x(0) = x$ and $p_x(T) = \nabla G(z_x(T))$, along with the optimality condition

$$\begin{aligned} u^*(t) &\in \arg \max_u \mathcal{H}(t, z_x(t), p_x(t), u) \\ &\iff \nabla_u \mathcal{H}(t, z_x, p_x, u^*) = 0. \end{aligned} \quad (5)$$

A classical and particularly effective way to exploit this structure is through its connection to dynamic programming. When the value function is sufficiently regular, the adjoint variable coincides with the gradient of the value function along optimal trajectories, thereby linking the PMP system to the Hamilton–Jacobi–Bellman (HJB) equation. This observation allows for a class of learning-based methods that parameterize the value function and recover feedback controls via Hamiltonian maximization. These types of approaches have demonstrated strong performance in high-dimensional optimal control problems (Onken et al., 2022; 2021a; Lin et al., 2021), particularly when the Hamiltonian

$$H(t, z_x, p_x) = \sup_u \mathcal{H}(t, z_x, p_x, u) \quad (6)$$

and the corresponding optimal controller u^* admit closed-form expressions (Onken et al., 2022; 2021a; Nakamura-Zimmerer et al., 2021; Zhao & Han, 2024; Verma et al., 2025). By embedding the structural relationships implied

by PMP directly into the learning process, value function parameterization can offer substantial efficiency gains over methods that directly parameterize the control policy (Onken et al., 2022; 2021a; Li et al., 2024). However, these advantages *critically depend* on the availability of an explicit Hamiltonian maximizer, which is often not the case in practical control problems.

1.1. Our Contribution

Recent work by (Gelphman et al., 2025) proposed an end-to-end framework for learning semi-global feedback controllers for (1) by directly parameterizing the value function. Their approach embeds the value function within an implicit neural network (El Ghaoui et al., 2021) and leverages Jacobian-Free Backpropagation (JFB) (Wu Fung et al., 2022) to enable efficient end-to-end training despite the presence of implicit Hamiltonians. The authors show promising empirical results for control problems of moderate dimensions. Their theoretical analysis establishes that JFB produces descent directions for *individual trajectories*. However, this *sample-wise* guarantee does not address the *stochastic* optimization setting. Critically, sample-wise descent does *not* imply convergence.

In this work, we extend that framework both theoretically and empirically. Our contributions are summarized as follows:

- **First convergence analysis for biased SGD in optimal control:** We prove that JFB-based stochastic gradient descent converges to stationary points when training over a distribution of trajectories, despite JFB producing *systematically biased* gradient estimates. This fundamentally differs from (Gelphman et al., 2025), which only established that individual sample updates move in descent directions.
- **Theoretical verification in practice:** We empirically verify that the assumptions required by our convergence analysis are satisfied in practical training regimes.
- **Scalability to 100-agent problems:** We demonstrate effectiveness on optimal control problems an order of magnitude larger than (Gelphman et al., 2025), including 100-agent consumption-savings, swarm quadrotor control, and multi-bicycle dynamics where standard implicit differentiation fails due to memory constraints (Section 5).

2. Related Works

Recent advances in neural network-based methods have enabled efficient solutions to high-dimensional optimal control

problems in settings where the Hamiltonian admits closed-form solutions. Approaches such as Neural-PMP (Gu et al., 2022), PMP-Net, and Pontryagin Differentiable Programming (Jin et al., 2020; 2021) leverage the Pontryagin Maximum Principle (PMP) to construct end-to-end differentiable frameworks for learning optimal controllers. Closely related are value function parameterization methods (Ruthotto et al., 2020; Li et al., 2024; Onken et al., 2022; 2021b;a; Verma et al., 2025; Lin et al., 2021; Vidal et al., 2023), which parameterize the value function directly and recover optimal controls via PMP relations. However, these approaches fundamentally rely on the ability to analytically solve the Hamiltonian maximization problem, which restricts their applicability when closed-form solutions are unavailable.

To address computational challenges in learning-based control, several differentiable optimization approaches have been proposed. DiffMPC (Amos et al., 2018) differentiates through Model Predictive Control via KKT conditions, while IDOC (Xu et al., 2023) achieves linear-time complexity through direct matrix equation evaluation. Learned MPC methods (Hertneck et al., 2018) further reduce computational cost using neural approximations, but often at the expense of preserving optimal control structure.

Most closely related to our work is the recent framework of (Gelphman et al., 2025), which introduced an implicit value function parameterization approach for optimal control problems with implicit Hamiltonians using implicit neural networks (INNs) and Jacobian-Free Backpropagation (JFB). While that work demonstrated promising empirical behavior and established sample-wise descent properties, it did not address stochastic minibatch training or convergence. This work extends this framework by developing a convergence theory for minibatch JFB and by providing a substantially broader empirical evaluation on high-dimensional optimal control problems.

3. Background

3.1. Optimal Control

A standard route to constructing optimal feedback controllers is through the system’s value function, denoted by $\phi(t, z)$. A key result in optimal control theory states that the value function fully characterizes the optimal control policy. In particular, along an optimal trajectory, the adjoint (costate) variable appearing in the Pontryagin Maximum Principle (PMP) coincides with the spatial gradient of the value function. More precisely, Theorem I.6.2 of (Fleming & Soner, 2006) states

$$p_x(t) = \nabla_z \phi(t, z_x^*(t)). \quad (7)$$

This relationship allows the optimal control defined implicitly by the PMP optimality condition (5) to be written

explicitly as a feedback law in terms of the value function,

$$u^*(t) = u^*(t, z_x^*(t), \nabla_z \phi(t, z_x^*(t))). \quad (8)$$

As a result, learning or approximating the value function immediately yields access to the associated optimal feedback controller.

The key difficulty addressed in this work arises at this stage. Evaluating the feedback law in (8) requires solving the Hamiltonian maximization problem in (5). When this maximization admits a closed-form solution, the resulting feedback law can be computed efficiently. However, in many problems of practical interest, no such closed-form expression exists (Betts, 2010; Gelfman et al., 2025). In these cases, computing u^* becomes computationally challenging, and existing value function-based approaches (Onken et al., 2022; 2021a; Meng et al., 2025; Ruthotto et al., 2020; Lin et al., 2021) become prohibitively expensive when the control dimension is large.

The value function ϕ itself satisfies the Hamilton–Jacobi–Bellman (HJB) partial differential equation (Evans, 2013),

$$-\partial_t \phi(t, z) + H(t, z, \nabla_z \phi(t, z)) = 0, \quad \phi(T, z) = G(z), \quad (9)$$

where the Hamiltonian H is obtained by solving the maximization problem in (6). This PDE formulation provides a complementary, dynamic-programming perspective on optimal control and further highlights the central role of the Hamiltonian maximization in both analysis and computation.

3.2. Implicit Deep Learning

To address the presence of implicit Hamiltonians in our control framework, we employ an Implicit Neural Network (INN) architecture. INNs define their outputs as fixed points of learnable operators (El Ghaoui et al., 2021). In our setting, the operator T_θ is constructed directly from the Hamiltonian optimality condition (5), and its fixed point corresponds to the optimal control. Specifically, the network output u_θ^* is defined implicitly through

$$u_\theta^* = T_\theta(u_\theta^*; t, z), \quad (10)$$

where $\theta \in \mathbb{R}^p$ denotes the network parameters and (t, z) are the input variables.

Unlike standard feedforward architectures, INNs are characterized by implicit fixed-point conditions (El Ghaoui et al., 2021; Wu Fung & Berkels, 2024). This modeling paradigm has been successfully applied across a wide range of applications, including optical flow estimation (Bai et al., 2022), game-theoretic equilibria (McKenzie et al., 2024a), maze-solving (Knutson et al., 2024), decision-focused learning (McKenzie et al., 2024b), image classification (Bai

et al., 2020), and inverse problems (Gilton et al., 2021; Yin et al., 2022; Liu et al., 2022; Heaton et al., 2021; Heaton & Wu Fung, 2023). Since the optimal control u^* in (5) is itself defined implicitly, INNs provide a natural modeling choice; that is, the fixed-point condition directly encodes the notion of optimality.

Training INNs typically requires differentiating through the solution of a fixed-point equation. A standard approach is implicit differentiation (He et al., 2016; El Ghaoui et al., 2021), obtained by differentiating both sides of (10),

$$\frac{du_\theta^*}{d\theta}(t, z) = \frac{\partial T_\theta(u_\theta^*; t, z)}{\partial u} \frac{du_\theta^*}{d\theta}(t, z) + \frac{\partial T_\theta(u_\theta^*; t, z)}{\partial \theta}.$$

Rearranging yields

$$\frac{du_\theta^*}{d\theta}(t, z) = \mathcal{J}_\theta^{-1} \frac{\partial T_\theta(u_\theta^*; t, z)}{\partial \theta}, \quad \mathcal{J}_\theta = I - \frac{\partial T_\theta(u_\theta^*; t, z)}{\partial u}, \quad (11)$$

which requires solving a linear system *for each evaluation of* (t, z) .

In the context of feedback control, this cost becomes prohibitive. *The linear system must be solved for every sample, at every time step (of a trajectory), and across all training iterations.* As a result, recent work has focused on reducing the computational burden of training implicit models (Bai et al., 2019; El Ghaoui et al., 2021; Wu Fung et al., 2022; Bolte et al., 2024). Among these methods, Jacobian-Free Backpropagation (JFB) (Wu Fung et al., 2022) offers a particularly simple alternative, closely related to one-step differentiation (Bolte et al., 2024). JFB replaces the Jacobian inverse \mathcal{J}_θ^{-1} with the identity, corresponding to a zeroth-order Neumann approximation,

$$\frac{du_\theta^*}{d\theta}(t, z) \approx \frac{\partial T_\theta(u_\theta^*; t, z)}{\partial \theta}. \quad (12)$$

Despite its simplicity, JFB has been shown to be effective in practice and is straightforward to implement (Wu Fung et al., 2022). An additional advantage of JFB is that it avoids difficulties associated with non-differentiable components in the operator T_θ , such as ReLU activations, making it particularly well suited for the control problems considered in this work.

3.3. Training Problem Formulation

We formulate training as an optimization over a distribution of initial conditions,

$$\min_{\theta} \mathbb{E}_{x \sim \rho} J_x(\theta) = \int_0^T L(s, z_x, u_\theta^*) ds + G(z_x(T)), \quad (13a)$$

$$\text{subject to: } \dot{z}_x = f(t, z_x, u_\theta^*), \quad z_x(0) = x, \quad (13b)$$

$$u_\theta^* \in \arg \max_u \mathcal{H}(t, z, \nabla \phi_\theta, u), \quad (13c)$$

where $\rho \in \mathbb{P}$ denotes a distribution over initial states defined on the probability space $\langle \Omega, \Sigma, P \rangle$, with P being the probability measure on the space. Solving (13a)–(13c) yields a semi-global value function and, consequently, a feedback controller, since training is performed over a family of initial conditions.

The main computational challenge lies in evaluating and differentiating through the implicitly defined control u_θ^* . As discussed in Section 3.2, u_θ^* is represented as the fixed point of an operator T_θ derived from the Hamiltonian optimality condition. For example, T_θ may be instantiated by an algorithmic update whose fixed points satisfy the first-order optimality condition om (13c), such as a gradient-based iteration, a proximal or operator-splitting scheme, or another monotone operator, while remaining differentiable with respect to the parameters θ . However, this implicit representation introduces nontrivial computational costs during training, since differentiation must account for the dependence of the fixed point on θ .

4. Convergence Analysis

4.1. Notation and Essential Assumptions

Assumption 4.1 (Smoothness and Contractivity). *The following holds.*

- (1) *There exists $\gamma \in (0, 1)$ such that the operator T_θ is γ -contractive in u for all $t \in [0, T]$, $z \in \mathbb{R}^n$ and $\theta \in \mathbb{R}^p$.*
- (2) *T_θ is C^1 with respect to θ, t, u, z . Furthermore, the gradient with respect to θ of the functional*

$$J_x[u_\theta] = \int_0^T L(t, u_\theta, z) dt + G(z(T)) \quad (14)$$

is L_J -Lipschitz and the functional (14) is bounded from below by a constant J_{\inf} in some open subset of its domain.

Definition 4.2 (Objective and Gradient and JFB). *The (true) gradient and JFB gradient approximation for a sample from the objective (13a)–(13c) as*

$$\nabla_\theta J_x = \int_0^T v_{\theta,x}(t) dt \quad \text{and} \quad d_x^{JFB} = \int_0^T w_{\theta,x}(t) dt, \quad (15)$$

respectively, where

$$v_{\theta,x}(t) = \frac{du_\theta^*}{d\theta}^\top h_{\theta,x}, \quad \text{and} \quad w_{\theta,x}(t) = \frac{\partial T_\theta}{\partial \theta}^\top h_{\theta,x}, \quad (16)$$

and $h_{\theta,x} = (\nabla_u L(t, z_x, u_\theta^) + \nabla_u f^\top p_x)$ represents the gradient of the Hamiltonian, p_x is the adjoint variable satisfying the adjoint equation (Evans, 2013), and $\frac{du_\theta^*}{d\theta}$ is the implicit gradient given by (11).*

Note that JFB *circumvents the expensive computation of $\frac{du_\theta^*}{d\theta}$* , and instead replaces it with $\frac{\partial T_\theta}{\partial \theta}$, resulting in significantly reduced computational cost.

For the remainder of this work, $\sigma_{\min}(\cdot)$ and $\sigma_{\max}(\cdot)$ are functions that, respectively, extract the smallest and largest singular values of its inputs, assumed to be a matrix.

Assumption 4.3 (Bound on Hamiltonian Gradient). *There exists $B_{\max} > 0$ such that for all t, z, θ , we have*

$$\|h_{\theta,x}(t, z, u_\theta^*)\| = \|\nabla_u L + \nabla_u f^\top p_x\| \leq B_{\max}, \quad (17)$$

where p_x is the adjoint variable satisfying the adjoint equations (Evans, 2013).

Assumption 4.3 requires the gradient of the Hamiltonian (with respect to the control) to be uniformly bounded above by B_{\max} .

Assumption 4.4 (Conditioning on JFB Integrand Matrix). *For any θ, t, z , the matrix $M_\theta = \frac{\partial T_\theta}{\partial \theta}(u_\theta^*; t, z) \in \mathbb{R}^{m \times p}$ has full row rank and satisfies the upper bound on the singular values*

$$\sigma_{\max}(M_\theta) \leq \frac{1}{\sqrt{\beta}}, \quad (18)$$

where $\beta > 0$. Moreover, the Gram matrix $M_\theta M_\theta^\top$ is non-singular and $(M_\theta M_\theta^\top)^{-1}$ satisfies the upper bound on the condition number

$$\kappa((M_\theta M_\theta)^{-1}) = \frac{\lambda_{\max}((M_\theta M_\theta)^{-1})}{\lambda_{\min}((M_\theta M_\theta)^{-1})} < \frac{1}{\gamma}. \quad (19)$$

Assumption 4.4 is based on the original paper on JFB (Wu Fung et al., 2022), which requires conditioning restrictions on the JFB update M_θ . For brevity, we denote $Var_x[v_{\theta,x}(t)] := \mathbb{E}_x[\|v_{\theta,x} - E_v\|^2]$ and similarly for $Var_x[w_{\theta,x}(t)] := \mathbb{E}_x[\|w_{\theta,x} - E_w\|^2]$.

Assumption 4.5 (Variance Bound). *$\forall \theta, t, z, \exists 0 < \delta_{var} < \lambda_- - \gamma \lambda_+$ such that*

$$\max(Var_x[v_{\theta,x}(t)], Var_x[w_{\theta,x}(t)])^2 \leq \delta_{var} \|\mathbb{E}_x[M_\theta v_{\theta,x}]\|^2, \quad (20)$$

where λ_+ and λ_- are uniform bounds on the largest and smallest eigenvalues of $M_\theta M_\theta^\top$ over θ, t, z , respectively.

Assumption 4.5 is possibly the most important assumption needed to prove convergence in expectation (and probability) to a critical point of (13a)–(13c). In words, this assumption controls how noisy the sample-wise integrands $v_{\theta,x}$ and $w_{\theta,x}$ are relative to their mean direction. This assumption is similar to variance bounds used standard proofs of stochastic gradient descent (SGD) (Bottou et al., 2018).

Assumption 4.6. *Let*

$$C_v = \frac{1}{T} \int_0^T v_{\theta,x}(t) dt \quad \text{and} \quad C_w = \frac{1}{T} \int_0^T w_{\theta,x}(t) dt, \quad (21)$$

where $v_{\theta,x}, w_{\theta,x}$ are defined in (16). We have that for all θ, x, z , the following hold.

- (1) Each element in the vectors $v_{\theta,x}, w_{\theta,x}$ is integrable on $[0, T]$ with respect to t . Moreover, $v_{\theta,x}, w_{\theta,x}$ are integrable on $[0, T] \times \Omega$, where Ω is the sample space of the distribution of initial conditions, ρ .
- (2) $\exists \delta_v, \delta_w, a_v, a_w \geq 0$ and $\epsilon_v > 0$ such that

$$\begin{aligned} \|\mathbb{E}_x[v_{\theta,x}(t) - C_v]\| &\leq a_v + \delta_v \|\mathbb{E}_x[\nabla_\theta J_x]\|, \\ \|\mathbb{E}_x[w_{\theta,x}(t) - C_w]\| &\leq a_w + \delta_w \|\mathbb{E}_x[d_x^{JFB}]\| \end{aligned}$$

and

$$\begin{aligned} \max(a_v + \delta_v \|\mathbb{E}_x[\nabla_\theta J_x]\|, a_w + \delta_w \|\mathbb{E}_x[d_x^{JFB}]\|)^2 \\ \leq \delta_\theta^2 - \frac{\epsilon_v}{T^2} \|\mathbb{E}_x[\nabla_\theta J_x]\|^2, \end{aligned}$$

where $\delta_\theta = \sqrt{\lambda_- - \gamma\lambda_+ - \delta_{var}} \|\mathbb{E}_x[M_\theta v_{\theta,x}(t)]\|$

Assumption 4.6 controls the magnitude of temporal deviations of the integrands from their time averages, which ensure that these deviations remain uniformly bounded. This condition captures a phenomenon specific to optimal control problems (the accumulation of gradient information over time) and does not arise in standard analysis of SGD.

4.2. Alignment of JFB and Gradient Lemmas

Lemma 4.7. *Under Assumptions 4.1-4.5,*

$$\langle \mathbb{E}_x[v_{\theta,x}(t)], \mathbb{E}_x[w_{\theta,x}(t)] \rangle \geq \delta_\theta^2 \geq 0, \quad \forall \theta, t, z.$$

Lemma 4.8. *Under Assumptions 4.1 - 4.6,*

$$\mathbb{E}_x[\nabla_\theta J_x]^\top \mathbb{E}_x[d_x^{JFB}] \geq \epsilon_v \|\mathbb{E}_x[\nabla_\theta J_x]\|^2, \quad \forall z, u, \theta.$$

The Lemmas above are particularly important because they show that the JFB update remains positively aligned with the true gradient in expectation, both pointwise in time and after time integration, which leads to descent of the expected objective. Proofs of both Lemmas can be found in the Section A of the Appendix.

4.3. Convergence of SGD Using JFB as the Stochastic Gradient

We begin by introducing notation to formalize the stochasticity arising in the training process. Let $\{\xi_j\}_{j \geq 0}$ denote a sequence of independent random variables representing the sampling procedure used to construct the JFB-based stochastic gradient. In particular, ξ_j corresponds to the random draw of initial conditions $x \sim \rho$ used to compute the JFB update at iteration j .

We analyze the convergence of SGD when the Jacobian-Free Backpropagation (JFB) direction is used as a stochastic gradient surrogate. Specifically, we consider the iterative scheme

$$\theta_{j+1} = \theta_j - \alpha_j d_{\xi_j}^{\text{JFB}}(\theta_j), \quad j \geq 0, \quad (22)$$

for minimizing the objective in (13a)–(13c) over $\theta \in \mathbb{R}^p$. Here, $d_{\xi_j}^{\text{JFB}}(\theta_j)$ denotes the JFB update computed using either a single sample or a minibatch of samples with corresponding learning rate α_j at iteration j .

Following the notation of (Bottou et al., 2018), we use $\mathbb{E}_{\xi_j}[\cdot]$ to denote the conditional expectation with respect to the randomness at iteration j , given the current iterate θ_j . Since θ_j depends on the sequence of random variables $\{\xi_0, \xi_1, \dots, \xi_{j-1}\}$, we also consider the total expectation of the objective with respect to all prior randomness, which we write as

$$\mathbb{E}[\mathbb{E}_x[J_x(\theta_j)]] = \mathbb{E}_{\xi_0} \left[\mathbb{E}_{\xi_1} \left[\dots \mathbb{E}_{\xi_{j-1}} \left[\mathbb{E}_x[J_x(\theta_j)] \right] \dots \right] \right]. \quad (23)$$

With this notation in place, we establish the following Lemma, which is used to prove the main result.

Lemma 4.9. *Under Assumptions 4.1 - 4.6, JFB-based SGD iterations (22) satisfy*

$$\begin{aligned} \mathbb{E}_{\xi_j}[\mathbb{E}_x[J_x(\theta_{j+1})]] - \mathbb{E}_x[J_x(\theta_j)] \leq \\ - \alpha_j \epsilon_v \|\mathbb{E}_x[\nabla_\theta J_x(\theta_j)]\|^2 + \frac{\alpha_j^2 L_J B_{\max}^2 T^2}{2\beta} \end{aligned}$$

With this result, the main results of this paper can be proven.

Theorem 4.10. *Suppose the sequence of learning rates $\{\alpha_j\}_{j=0}^\infty$ is monotonically decreasing and satisfies $\sum_{j=0}^\infty \alpha_j = \infty$, $\sum_{j=0}^\infty \alpha_j^2 < \infty$, and $0 < \alpha_0 \leq \frac{2\epsilon_v}{L_J(1-\gamma)^2}$. Let $A_K = \sum_{j=0}^K \alpha_j$. Then, under Assumptions 4.1- 4.6, the JFB-based SGD iteration (22) satisfies*

$$\lim_{K \rightarrow \infty} \mathbb{E} \left[\frac{1}{A_K} \sum_{j=0}^K \alpha_j \|\mathbb{E}_x[\nabla_\theta J_x(\theta_j)]\|^2 \right] = 0.$$

In words, the weighted Cesaro sum of the sequence $\{\|\mathbb{E}_x[\nabla_\theta J_x(\theta_j)]\|^2\}_{j=0}^\infty$ converges in (total) expectation to 0. Using Theorem 4.10, one can then use standard SGD analysis to show the following theorem and corollary.

Theorem 4.11. *Under the assumptions of Theorem 4.10, the JFB-based SGD iteration (22) satisfies*

$$\liminf_{j \rightarrow \infty} \mathbb{E} \left[\|\mathbb{E}_x[\nabla_\theta J_x(\theta_j)]\|^2 \right] = 0.$$

Using Theorem 4.10, we can also prove convergence in probability to a critical point.

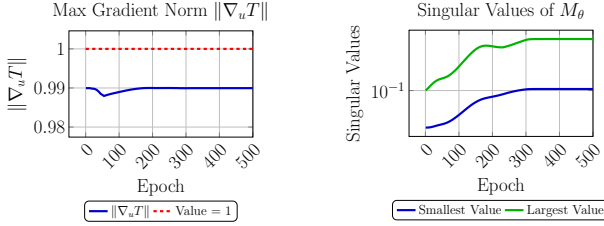


Figure 1. Numerical verification on quadrotor experiment. (Left) Maximum singular value of the Jacobian of the operator T_θ , evaluated on the worst-case sample within each minibatch, illustrating that the operator remains contractive throughout training. (Right) Smallest and largest singular values of M_θ , computed batch-wise over all time steps for the single quadrotor experiment, confirming the full row-rank property of M_θ and the boundedness of $\sigma_{\max}(M_\theta)$.

Corollary 4.12. Suppose the assumptions of Theorem 4.10 hold. For any $K \in \mathbb{N}$ let $j(K) \in \{0, 1, \dots, K\}$ represent a random index chosen with probabilities proportional to $\{\alpha_j\}_{j=0}^K$. Then, $\{\|\mathbb{E}_x[\nabla_\theta J_x(\theta_j)]\|\}_{j=0}^K \rightarrow 0$ as $K \rightarrow \infty$ in probability.

Finally, we note that it is possible to relax Assumption 4.5 and instead obtain convergence to a *neighborhood* of the stationary point instead C.4. See Section C for more details.

5. Experiments

We first empirically verify the assumptions underlying our convergence analysis that can be evaluated directly in practice. We then compare JFB with existing backpropagation methods for implicit neural networks on low- to moderate-dimensional benchmarks. Finally, we demonstrate the effectiveness and scalability of the proposed approach on a range of high-dimensional optimal control problems, including optimal multi-agent consumption–savings and multi-agent quadrotor and bicycle control. In the quadrotor and consumption–savings settings, the use of an exponential running cost leads to an implicit H (see Section B for a description of consumption savings Hamiltonian), while in the multi-agent bicycle problem, the nonlinearity of the dynamics automatically renders H implicit. While the quadrotor and multi-bicycle dynamics are well established, the optimal consumption–savings model is less standard; we therefore provide a detailed description of this problem in Appendix B.

For concreteness, we instantiate the fixed-point operator T_θ using a simple gradient-based update derived from the Hamiltonian optimality condition; however, our theoretical results apply more broadly to general choices of T_θ that satisfy the stated assumptions.

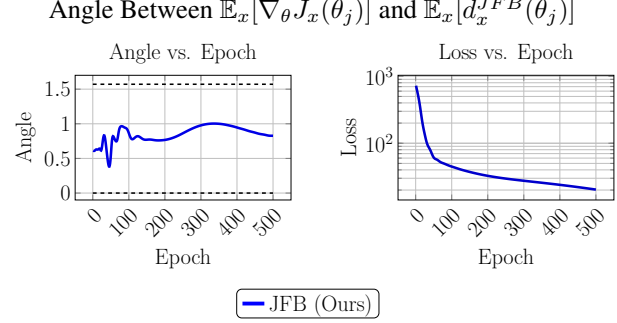


Figure 2. Angle between $\mathbb{E}_x[\nabla_\theta J_x]$ and $\mathbb{E}_x[d_x^{JFB}]$ (Left) plotted alongside loss vs. epoch (Right). The values plotted are the largest batch-wise angles. $\mathbb{E}_x[\nabla_\theta J_x]$ is computed using AD. The dashed lines are at the angles 0 and $\frac{\pi}{2}$.

5.1. Theoretical Verification

To empirically verify key theoretical properties of JFB, we consider an optimal control task involving a single quadrotor. We focus on assumptions from the convergence analysis that can be evaluated directly during training, without requiring access to the true optimal solution or adjoint variable.

Contractivity. We examine whether the operator T_θ , instantiated via a gradient-based update with fixed stepsize 0.01 to solve (13c), is contractive. Since the contractivity factor depends on the learned parameters θ , this property cannot be directly enforced and must instead be verified empirically. As shown in Figure 1, the operator remains contractive at every training iteration, where the reported gradient corresponds to the worst-case sample within each minibatch. Notably, the network consistently learns parameters that preserve contractivity throughout training.

Rank and Conditioning of M_θ . Next, we examine the full-rank condition and boundedness of the largest singular value of M_θ appearing in Assumption 4.4. As shown in Figure 1, the singular values of M_θ remain bounded above and bounded away from zero throughout training, which ensures that M_θ retains full rank. Consequently, $\lambda_{\max}((M_\theta M_\theta^\top)^{-1})$ remains bounded above and $\lambda_{\min}((M_\theta M_\theta^\top)^{-1})$ is bounded away from zero.

Descent Verification. We verify that JFB produces a descent direction in practice. For each minibatch, we compute both the average JFB update and the corresponding average of the true gradients, and evaluate the angle between them. As shown in Figure 2 (left panel), this angle remains strictly between 0 and $\pi/2$ throughout training, indicating consistent alignment. In particular, the angle between $\mathbb{E}_x[\nabla_\theta J_x]$ and $\mathbb{E}_x[d_x^{JFB}]$ remains well within $[0, \pi/2]$, which implies that the inner product $\mathbb{E}_x[\nabla_\theta J_x]^\top \mathbb{E}_x[d_x^{JFB}]$ is uniformly bounded away from zero.

While it is not practical to verify each remaining assumption

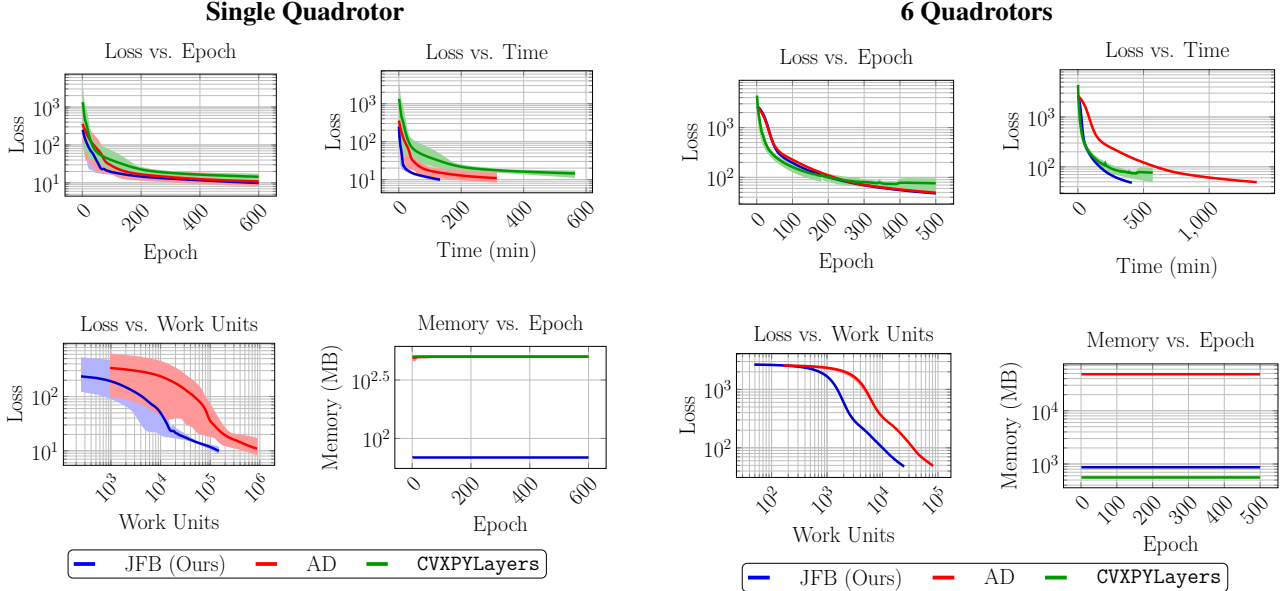


Figure 3. Comparison of JFB, automatic differentiation (AD), and CVXPYLayers (Agrawal et al., 2019) (Implicit Differentiation) for training the value function for a quadrotor across four metrics. (Top Left) Loss versus training epochs. (Top Right) Loss plotted against cumulative runtime in minutes. (Bottom Left) Loss plotted against cumulative work units, with one work unit being one evaluation of $\frac{\partial T_\theta}{\partial \theta}$, which is equivalent to backpropagation through one application of T_θ . (Bottom Right) Maximum GPU memory usage per training epoch.

leading to Lemma 4.9 individually, we instead demonstrate a consistent decrease in the training loss (right panel of Figure 2). This observed descent provides empirical evidence that the remaining assumptions are reasonable in practice and that the conclusion of Lemma 4.9 holds. Accordingly, the angle and descent checks presented here constitute the most meaningful empirical validation of the theory, as they directly assess whether the stochastic JFB updates act as descent directions.

5.2. Comparison in Low- and Moderate-Dimensional Settings

We compare several implicit deep learning approaches, including the proposed JFB method, CVXPYLayers (Agrawal et al., 2019), and traditional automatic differentiation (AD) (Paszke et al., 2019). To ensure a fair comparison, we focus on low- and moderate-dimensional problems, specifically, single-quadrotor and six-quadrotor control tasks, which remain tractable for all methods. For all experiments, learning rates were chosen to yield the best empirical performance. We used a fixed learning rate of 0.001 for the single-quadrotor task, and a ReduceLROnPlateau scheduler with initial learning rate 0.01, decay factor 0.5, and patience 10 for the six-quadrotor task.

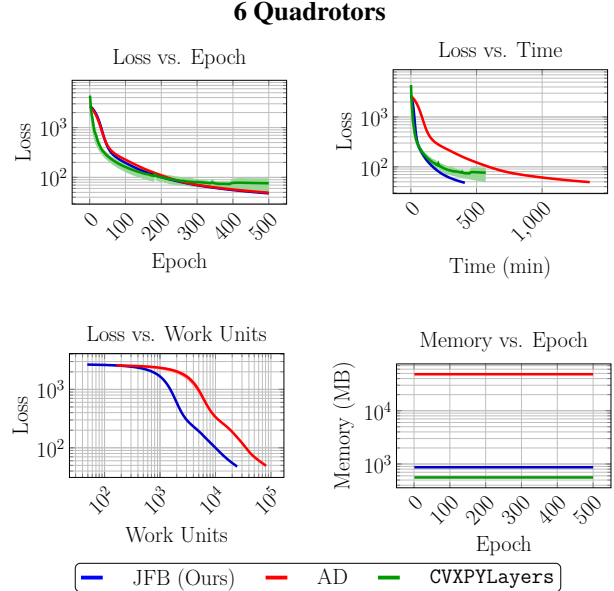


Figure 4. Comparison of JFB, automatic differentiation (AD), and CVXPYLayers (Implicit Differentiation) for training the value function for 6 quadrotors across three metrics. (Top Left) Loss versus training epochs. (Top Right) Loss plotted against cumulative runtime in minutes. (Bottom Left) Loss plotted against cumulative work units. (Bottom Right) Maximum GPU memory usage per training epoch.

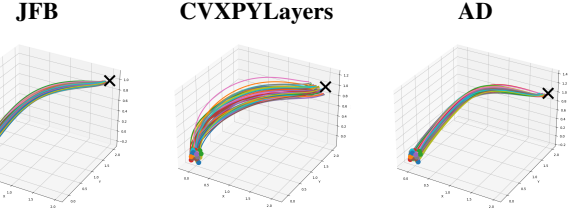


Figure 5. Trajectories of trained quadrotors using JFB (left panel), CVXPYLayers (middle panel), and AD (right panel).

As shown in Figures 3 and 4, all methods exhibit comparable loss trajectories when measured against training epochs (top left panels). However, JFB converges substantially faster when performance is evaluated against wall-clock time (top right panels). This efficiency arises from avoiding both the storage of fixed-point iterations required by AD (bottom right) and the per-time-step linear solves required by CVXPYLayers. In addition, we visualize the resulting position trajectories for the quadrotor problem in Figure 5, which shows that JFB produces trajectories that are qualitatively comparable to those obtained using automatic differentiation and noticeably closer to the target than those obtained using CVXPYLayers.

To provide a fairer comparison between AD and JFB, we also report loss versus *work units*, defined as the number of applications of $\partial T_\theta / \partial \theta$ (bottom left panels). We do not

Table 1. Final Control Objective (13a)-(13c) Comparison for Low- and Moderate-dimensional Problems.

	AD	CVXPYLayers	JFB
Single Quadrotor	37.720	93.653	30.406
Six Quadrotors	72.846	39.458	24.150

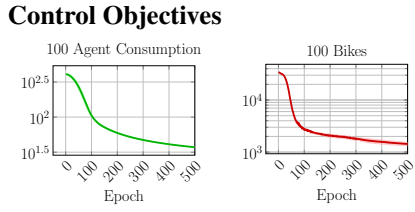


Figure 6. Training trajectories of the control objective (13a)-(13c) for the high-dimensional problems using JFB. Solid lines show the mean over three runs, with shaded regions indicating the best and worst values per epoch. The memory required per epoch is as follows. For both 100 quadrotors and 100 bicycles, JFB uses 36287.0 MB vRAM per epoch. For 100 agent consumption savings, JFB uses 5411.0 MB vRAM per epoch.

report this metric for CVXPYLayers, as its gradient computations are performed entirely as a black box; however, the reported runtimes indicate that it is likely less efficient than JFB but more efficient than AD. Finally, we note that the six-quadrotor setting represents the highest-dimensional problem that could be solved using AD before encountering memory limitations. Finally, Table 1 reports the final control objective values after training for both the single- and six-quadrotor experiments. While all methods achieve comparable final losses, JFB reaches these solutions with substantially faster runtimes and fewer work units its computational efficiency.

5.3. High-Dimensional Experiments

We next highlight the effectiveness of JFB on high-dimensional optimal control problems with implicit Hamiltonians. Traditional automatic differentiation (AD) is *infeasible* in these settings due to excessive memory consumption, as it requires storing every application of T_θ within the computational graph (see (Wu Fung et al., 2022) for a detailed discussion). CVXPYLayers is similarly *infeasible* for the consumption–savings and bicycle problems, since neither admits dynamics that are linear in the control variable u , and is prohibitively slow for the 100-quadrotor experiment. In contrast, JFB enables us to train these networks and approximate solutions for all three high-dimensional problems, as seen Figure 6 while also maintaining *constant* memory per epoch. Here, the 100 quadrotor problem is 1200-dimensional in the state and 400-dimensional in the controller. The 100 agent consumption problem is 100-dimensional in both state and controller. The 100 bikes are 400-dimensional in the state and 200-dimensional in the

controller.

All high-dimensional experiments employed PyTorch’s ReduceLROnPlateau learning rate scheduler with a decay factor of 0.5 and patience of 10. Additional hyperparameters, such as batch size, were tuned individually for each experiment to achieve the lowest control objective.

6. Discussion

This work provides the first convergence theory for training implicit neural networks in optimal control problems with implicit Hamiltonians using a biased stochastic gradient method, namely Jacobian-Free Backpropagation (JFB). Our analysis shows that, despite the bias introduced by ignoring Jacobian inversion *at each time step, and for each trajectory* in the gradient estimate, we can ensure convergence under standard smoothness, contractivity, and variance assumptions. Empirically, we demonstrate that key theoretical conditions, such as contractivity, conditioning of M_θ , and descent, can be monitored during training, and that JFB scales effectively to high-dimensional control problems where AD and optimization-based methods are infeasible.

Limitations. The primary limitation of this work is its reliance on the contractivity of the operator T_θ . Although we empirically observe this property to hold in our experiments, contractivity may fail for more sophisticated optimization schemes used to evaluate (13c), as well as in settings where the Hamiltonian \mathcal{H} is only locally, rather than strongly, concave. Consequently, an important direction for future work is to extend the convergence analysis to non-contractive or averaged operators. In addition, relaxing the analysis to accommodate cases in which u_θ^* corresponds to a local maximizer of \mathcal{H} would further broaden the applicability of the framework.

7. Conclusion

We develop the first convergence guarantees for Jacobian-Free Backpropagation (JFB) as a biased stochastic gradient method in optimal control problems with implicit Hamiltonians. Our results show that JFB converges to stationary points despite the absence of exact gradient information and enable scalable learning in high-dimensional control settings. Together, the theory and experiments establish JFB as a principled and practical approach for learning value function–based feedback controllers when closed-form Hamiltonians are unavailable. Future work will extend this framework to mean-field control/games settings (Lasry & Lions, 2007; Vidal et al., 2025; Agrawal et al., 2022; Laurière et al., 2022; Wang et al., 2025; Chow et al., 2022; Yang & Ichiba, 2023), where the scalability of our approach may prove useful. Code for this work will be provided upon publication.

References

Agrawal, A., Amos, B., Barratt, S., Boyd, S., Diamond, S., and Kolter, J. Z. Differentiable convex optimization layers. *Advances in neural information processing systems*, 32, 2019.

Agrawal, S., Lee, W., Wu Fung, S., and Nurbekyan, L. Random features for high-dimensional nonlocal mean-field games. *Journal of Computational Physics*, 459: 111136, 2022.

Amos, B., Jimenez, I., Sacks, J., Boots, B., and Kolter, J. Z. Differentiable mpc for end-to-end planning and control. *Advances in neural information processing systems*, 31, 2018.

Bai, S., Kolter, J. Z., and Koltun, V. Deep Equilibrium Models. *Advances in Neural Information Processing Systems*, 32, 2019.

Bai, S., Koltun, V., and Kolter, J. Z. Multiscale Deep Equilibrium Models. *Advances in Neural Information Processing Systems*, 33:5238–5250, 2020.

Bai, S., Geng, Z., Savani, Y., and Kolter, J. Z. Deep equilibrium optical flow estimation. In *Proceedings of the IEEE/CVF conference on computer vision and pattern recognition*, pp. 620–630, 2022.

Betts, J. T. *Practical methods for optimal control and estimation using nonlinear programming*. SIAM, 2010.

Bolte, J., Pauwels, E., and Vaiter, S. One-step differentiation of iterative algorithms. *Advances in Neural Information Processing Systems*, 36, 2024.

Bottou, L., Curtis, F. E., and Nocedal, J. Optimization methods for large-scale machine learning. *SIAM review*, 60(2):223–311, 2018.

Chow, Y. T., Wu Fung, S., Liu, S., Nurbekyan, L., and Osher, S. A numerical algorithm for inverse problem from partial boundary measurement arising from mean field game problem. *Inverse Problems*, 39(1):014001, 2022.

Demidovich, Y., Malinovsky, G., Sokolov, I., and Richtarik, P. A Guide Through the Zoo of Biased Stochastic Gradient Descent. *Advances in Neural Information Processing Systems*, 36, 2024.

El Ghaoui, L., Gu, F., Travacca, B., Askari, A., and Tsai, A. Implicit deep learning. *SIAM Journal on Mathematics of Data Science*, 3(3):930–958, 2021.

Evans, L. C. An introduction to mathematical optimal control theory version 0.2, 2013.

Fleming, W. H. and Soner, H. M. *Controlled Markov processes and viscosity solutions*, volume 25. Springer Science & Business Media, 2006.

Gelphman, E., Verma, D., Yang, N. T., Osher, S., and Fung, S. W. End-to-end training of high-dimensional optimal control with implicit hamiltonians via jacobian-free back-propagation. *arXiv preprint arXiv:2510.00359*, 2025.

Gilton, D., Ongie, G., and Willett, R. Deep Equilibrium Architectures for Inverse Problems in Imaging. *IEEE Transactions on Computational Imaging*, 7:1123–1133, 2021.

Gu, C., Xiong, H., and Chen, Y. Pontryagin optimal control via neural networks. *arXiv preprint arXiv:2212.14566*, 2022.

He, K., Zhang, X., Ren, S., and Sun, J. Deep residual learning for image recognition. In *IEEE Conference on Computer Vision and Pattern Recognition (CVPR)*, pp. 770–778, 2016.

Heaton, H. and Wu Fung, S. Explainable ai via learning to optimize. *Scientific Reports*, 13(1):10103, 2023.

Heaton, H., Wu Fung, S., Gibali, A., and Yin, W. Feasibility-based fixed point networks. *Fixed Point Theory and Algorithms for Sciences and Engineering*, 2021:1–19, 2021.

Hertneck, M., Köhler, J., Trimpe, S., and Allgöwer, F. Learning an approximate model predictive controller with guarantees. *IEEE Control Systems Letters*, 2(3):543–548, 2018.

Jin, W., Wang, Z., Yang, Z., and Mou, S. Pontryagin differentiable programming: An end-to-end learning and control framework. *Advances in Neural Information Processing Systems*, 33:7979–7992, 2020.

Jin, W., Mou, S., and Pappas, G. J. Safe pontryagin differentiable programming. *Advances in Neural Information Processing Systems*, 34:16034–16050, 2021.

Knutson, B., Rabeendran, A. C., Ivanitskiy, M., Pettyjohn, J., Diniz-Behn, C., Wu Fung, S., and McKenzie, D. On logical extrapolation for mazes with recurrent and implicit networks. *arXiv preprint arXiv:2410.03020*, 2024.

Kopp, R. E. Pontryagin maximum principle. In *Mathematics in Science and Engineering*, volume 5, pp. 255–279. Elsevier, 1962.

Lasry, J.-M. and Lions, P.-L. Mean field games. *Japanese journal of mathematics*, 2(1):229–260, 2007.

Laurière, M., Perrin, S., Pérolat, J., Girgin, S., Muller, P., Élie, R., Geist, M., and Pietquin, O. Learning in mean field games: A survey. *arXiv preprint arXiv:2205.12944*, 2022.

Li, X., Verma, D., and Ruthotto, L. A neural network approach for stochastic optimal control. *SIAM Journal on Scientific Computing*, 46(5):C535–C556, 2024.

Lin, A. T., Wu Fung, S., Li, W., Nurbekyan, L., and Osher, S. J. Alternating the population and control neural networks to solve high-dimensional stochastic mean-field games. *Proceedings of the National Academy of Sciences*, 118(31):e2024713118, 2021.

Liu, J., Xu, X., Gan, W., Kamilov, U., et al. Online deep equilibrium learning for regularization by denoising. *Advances in Neural Information Processing Systems*, 35: 25363–25376, 2022.

McKenzie, D., Heaton, H., Li, Q., Wu Fung, S., Osher, S., and Yin, W. Three-Operator Splitting for Learning to Predict Equilibria in Convex Games. *SIAM Journal on Mathematics of Data Science*, 6(3):627–648, 2024a.

McKenzie, D., Wu Fung, S., and Heaton, H. Differentiating Through Integer Linear Programs with Quadratic Regularization and Davis-Yin Splitting. *Transactions on Machine Learning Research*, 2024b.

Meng, T., Liu, S., Wu Fung, S., and Osher, S. Recent advances in numerical solutions for Hamilton-Jacobi PDEs. *arXiv preprint arXiv:2502.20833*, 2025.

Nakamura-Zimmerer, T., Gong, Q., and Kang, W. Adaptive deep learning for high-dimensional Hamilton-Jacobi–Bellman equations. *SIAM Journal on Scientific Computing*, 43(2):A1221–A1247, 2021.

Onken, D., Nurbekyan, L., Li, X., Wu Fung, S., Osher, S., and Ruthotto, L. A neural network approach applied to multi-agent optimal control. In *2021 European Control Conference (ECC)*, pp. 1036–1041. IEEE, 2021a.

Onken, D., Wu Fung, S., Li, X., and Ruthotto, L. Ottflow: Fast and accurate continuous normalizing flows via optimal transport. In *Proceedings of the AAAI Conference on Artificial Intelligence*, volume 35, 2021b.

Onken, D., Nurbekyan, L., Li, X., Wu Fung, S., Osher, S., and Ruthotto, L. A neural network approach for high-dimensional optimal control applied to multiagent path finding. *IEEE Transactions on Control Systems Technology*, 31(1):235–251, 2022.

Paszke, A., Gross, S., Massa, F., Lerer, A., Bradbury, J., Chanan, G., Killeen, T., Lin, Z., Gimelshein, N., Antiga, L., et al. PyTorch: An Imperative Style, High-Performance Deep Learning Library. *Advances in neural information processing systems*, 32, 2019.

Pontryagin, L. S. *Mathematical theory of optimal processes*. Routledge, 2018.

Ruthotto, L., Osher, S. J., Li, W., Nurbekyan, L., and Wu Fung, S. A machine learning framework for solving high-dimensional mean field game and mean field control problems. *Proceedings of the National Academy of Sciences*, 117(17):9183–9193, 2020.

Verma, D., Winovich, N., Ruthotto, L., and van Bloemen Waanders, B. Neural network approaches for parameterized optimal control. *Foundations of Data Science*, 7(1):363–385, 2025. doi: 10.3934/fods.2024042. URL <https://www.aimscolleges.org/article/id/66ea8ba12bcf34161cd88c93>.

Vidal, A., Wu Fung, S., Tenorio, L., Osher, S., and Nurbekyan, L. Taming hyperparameter tuning in continuous normalizing flows using the jko scheme. *Scientific reports*, 13(1):4501, 2023.

Vidal, A., Fung, S. W., Osher, S., Tenorio, L., and Nurbekyan, L. Kernel expansions for high-dimensional mean-field control with non-local interactions. In *2025 American Control Conference (ACC)*, pp. 4164–4171. IEEE, 2025.

Wang, X., Fung, S. W., and Nurbekyan, L. A primal-dual price-optimization method for computing equilibrium prices in mean-field games models. *arXiv preprint arXiv:2506.04169*, 2025.

Wu Fung, S. and Berkels, B. A generalization bound for a family of implicit networks. *arXiv preprint arXiv:2410.07427*, 2024.

Wu Fung, S., Heaton, H., Li, Q., McKenzie, D., Osher, S., and Yin, W. JFB: Jacobian-Free Backpropagation for Implicit Networks. In *Proceedings of the AAAI Conference on Artificial Intelligence*, volume 36, pp. 6648–6656, 2022.

Xu, M., Molloy, T. L., and Gould, S. Revisiting implicit differentiation for learning problems in optimal control. *Advances in Neural Information Processing Systems*, 36: 60060–60076, 2023.

Yang, N. T. and Ichiba, T. Relative arbitrage opportunities in an extended mean field system. *arXiv preprint arXiv:2311.02690*, 2023.

Yin, W., McKenzie, D., and Wu Fung, S. Learning to Optimize: Where Deep Learning Meets Optimization and Inverse Problems. *SIAM News*, 2022.

Zhao, Y. and Han, J. Offline supervised learning vs online direct policy optimization: A comparative study and a unified training paradigm for neural network-based optimal feedback control. *Physica D: Nonlinear Phenomena*, 462:134130, 2024.

A. Proof of Main Result

In this section, we provide proofs to all the Lemmas and Theorems. For ease of presentation, we re-state the Lemmas and Theorems before proving them.

A.1. Proof of Lemma 4.7

Lemma 4.7: Under Assumptions 4.1-4.5,

$$\langle \mathbb{E}_x[v_{\theta,x}(t)], \mathbb{E}_x[w_{\theta,x}(t)] \rangle \geq \delta_\theta^2 \geq 0, \quad \forall \theta, t, z.$$

Proof. Outline of Proof: The proof is carried out in four main steps.

Step 1. Fixing x , reformulate $\langle v_{\theta,x}, w_{\theta,x} \rangle$ in terms of $M_\theta v_{\theta,x}$.

Step 2. Use this new formulation and the given assumptions to derive the single-sample (no expectation with respect to x) form of desired inequality.

Step 3. Take expectation with respect to x on both sides of the result of Step 2 and apply Jensen's inequality.

Step 4. Using Assumption 4.5, algebraically rearrange the result of Step 3 to obtain the desired result.

Step 1: Let $\psi := M_\theta v_{\theta,x}$. Substituting the definition of $v_{\theta,x}$:

$$\psi = M_\theta(M_\theta^\top \mathcal{J}_\theta^{-\top} h_{\theta,x}) = (M_\theta M_\theta^\top) \mathcal{J}_\theta^{-\top} h_{\theta,x}. \quad (24)$$

By Assumption 4.4, $M_\theta M_\theta^\top$ is nonsingular. The matrix \mathcal{J}_θ , and therefore $\mathcal{J}_\theta^{-\top}$, is assumed to be nonsingular.

Our goal is to express $\langle v_{\theta,x}, w_{\theta,x} \rangle$ in terms of ψ . Given $\psi = (M_\theta M_\theta^\top) \mathcal{J}_\theta^{-\top} h_{\theta,x}$, we have

$$h_{\theta,x} = \mathcal{J}_\theta^\top (M_\theta M_\theta^\top)^{-1} \psi. \quad (25)$$

Substituting this back into the definitions, we obtain

$$\begin{aligned} v_{\theta,x} &= M_\theta^\top \mathcal{J}_\theta^{-\top} [\mathcal{J}_\theta^\top (M_\theta M_\theta^\top)^{-1} \psi] = M_\theta^\top (M_\theta M_\theta^\top)^{-1} \psi \\ w_{\theta,x} &= M^\top [\mathcal{J}_\theta^\top (M_\theta M_\theta^\top)^{-1} \psi] = M^\top \mathcal{J}_\theta^\top (M_\theta M_\theta^\top)^{-1} \psi \end{aligned}$$

Therefore, $\langle v_{\theta,x}, w_{\theta,x} \rangle = \langle \psi, \mathcal{J}_\theta^\top (M_\theta M_\theta^\top)^{-1} \psi \rangle$, using the definition of adjoint.

Step 2: Let $A = (M_\theta M_\theta^\top)^{-1}$. Since $M_\theta M_\theta^\top$ is symmetric positive definite, so is A . Let λ_+ and λ_- denote the largest and smallest eigenvalues of A , and define $\bar{\lambda} = \frac{1}{2}(\lambda_+ + \lambda_-)$.

Using the assumptions of this Lemma, we have by Lemma A-1 in the original JFB paper (Fung et. al. 2022), \mathcal{J}_θ^\top is coercive, that is, $\langle \psi, \mathcal{J}_\theta^\top \psi \rangle \geq (1 - \gamma) \|\psi\|^2$. Using this and Cauchy-Schwarz,

$$\begin{aligned} \langle \psi, \mathcal{J}_\theta^\top A \psi \rangle &= \langle \psi, \mathcal{J}_\theta^\top (\bar{\lambda} I + A - \bar{\lambda} I) \psi \rangle \\ &= \bar{\lambda} \langle \psi, \mathcal{J}_\theta^\top \psi \rangle + \langle \psi, \mathcal{J}_\theta^\top (A - \bar{\lambda} I) \psi \rangle \\ &\geq \bar{\lambda}(1 - \gamma) \|\psi\|^2 - \|\mathcal{J}_\theta^\top\| \|A - \bar{\lambda} I\| \|\psi\|^2. \end{aligned}$$

Using Lemmas A-1 and A-2 from Wu Fung et. al. 2022, we have $\|\mathcal{J}_\theta^\top\| \leq 1 + \gamma$ and $\|A - \bar{\lambda} I\| = \frac{1}{2}(\lambda_+ - \lambda_-)$. Substituting these gives,

$$\langle v_{\theta,x}, w_{\theta,x} \rangle \geq \left[\frac{\lambda_+ + \lambda_-}{2} (1 - \gamma) - (1 + \gamma) \frac{\lambda_+ - \lambda_-}{2} \right] \|\psi\|^2.$$

By Assumption 4.4 the condition number $\kappa(A) < \frac{1}{\gamma} \implies (\lambda_- - \gamma \lambda_+) > 0$. Thus, we have $\langle v_{\theta,x}, w_{\theta,x} \rangle \geq \|\psi\|^2 (\lambda_- - \gamma \lambda_+) \geq 0$.

Step 3: Taking the expectation with respect to x on both sides of the result of Step 2 and using $\psi = M_\theta v_{\theta,x}$ we have

$$\begin{aligned}\mathbb{E}_x[\langle v_{\theta,x}, w_{\theta,x} \rangle] &\geq \mathbb{E}_x[(\lambda_- - \gamma\lambda_+) \|M_\theta v_{\theta,x}\|^2] \\ \mathbb{E}_x[\langle v_{\theta,x}, w_{\theta,x} \rangle] &\geq (\lambda_- - \gamma\lambda_+) \mathbb{E}_x[\|M_\theta v_{\theta,x}\|^2] \\ \mathbb{E}_x[\langle v_{\theta,x}, w_{\theta,x} \rangle] &\geq (\lambda_- - \gamma\lambda_+) \|\mathbb{E}_x[M_\theta v_{\theta,x}]\|^2\end{aligned}$$

where the last line above is due to Jensen's inequality.

Step 4: Let $E_v = \mathbb{E}_x[v_{\theta,x}]$, $E_w = \mathbb{E}_x[w_{\theta,x}]$. Rewriting $\mathbb{E}_x[\langle v_{\theta,x}, w_{\theta,x} \rangle]$,

$$\begin{aligned}\mathbb{E}_x[\langle v_{\theta,x}, w_{\theta,x} \rangle] &= \mathbb{E}_x[\langle v_{\theta,x} - E_v + E_v, w_{\theta,x} - E_w + E_w \rangle] \\ &= \mathbb{E}_x[\langle v_{\theta,x} - E_v, w_{\theta,x} - E_w \rangle] + \langle \mathbb{E}_x[v_{\theta,x} - E_v], E_w \rangle \\ &\quad + \langle E_v, \mathbb{E}_x[w_{\theta,x} - E_w] \rangle + \langle E_v, E_w \rangle \\ &= \mathbb{E}_x[\langle v_{\theta,x} - E_v, w_{\theta,x} - E_w \rangle] + \langle 0, E_w \rangle + \langle E_w, 0 \rangle + \langle E_v, E_w \rangle \\ &= \mathbb{E}_x[\langle v_{\theta,x} - E_v, w_{\theta,x} - E_w \rangle] + \langle E_v, E_w \rangle\end{aligned}$$

By the Cauchy-Schwarz inequality, the last line above becomes

$$\begin{aligned}\mathbb{E}_x[\langle v_{\theta,x}, w_{\theta,x} \rangle] &\leq \sqrt{\mathbb{E}_x[\|v_{\theta,x} - E_v\|^2]} \sqrt{\mathbb{E}_x[\|w_{\theta,x} - E_w\|^2]} + \langle E_v, E_w \rangle \\ &\leq \sqrt{\text{Var}_x[v_{\theta,x}]} \sqrt{\text{Var}_x[w_{\theta,x}]} + \langle E_v, E_w \rangle \\ &\leq \max \left(\sqrt{\text{Var}_x[v_{\theta,x}]}, \sqrt{\text{Var}_x[w_{\theta,x}]} \right)^2 + \langle E_v, E_w \rangle \\ &\leq \delta_{var} \|\mathbb{E}_x[M_\theta v_{\theta,x}]\|^2 + \langle E_v, E_w \rangle\end{aligned}$$

Rearranging the last line above and applying the result of Step 3 yields

$$\langle E_v, E_w \rangle \geq \mathbb{E}_x[\langle v_{\theta,x}, w_{\theta,x} \rangle] - \delta_{var} \|\mathbb{E}_x[M_\theta v_{\theta,x}]\|^2 \quad (26)$$

$$\geq (\lambda_- - \gamma\lambda_+) \|\mathbb{E}_x[M_\theta v_{\theta,x}]\|^2 - \delta_{var} \|\mathbb{E}_x[M_\theta v_{\theta,x}]\|^2 \quad (27)$$

$$\geq (\lambda_- - \gamma\lambda_+ - \delta_{var}) \|\mathbb{E}_x[M_\theta v_{\theta,x}]\|^2 \quad (28)$$

$$= \delta_\theta^2 \geq 0 \quad (29)$$

□

A.2. Proof of Lemma 4.8

Lemma 4.8: Under Assumptions 4.1 - 4.6,

$$\mathbb{E}_x[\nabla_\theta J_x]^\top \mathbb{E}_x[d_x^{JFB}] \geq \epsilon_v \|\mathbb{E}_x[\nabla_\theta J_x]\|^2, \quad \forall z, u, \theta.$$

Proof. Let $E_1 = \mathbb{E}_x[\nabla_\theta J_x]$ and $E_2 = \mathbb{E}_x[d_x^{JFB}]$ so $E_1^\top E_2 = T^2 \mathbb{E}_x[C_v]^\top \mathbb{E}_x[C_w]$. We have that

$$\int_0^T \mathbb{E}_x[v_{\theta,x}(t)]^\top \mathbb{E}_x[w_{\theta,x}(t)] dt \quad (30)$$

$$= \int_0^T \mathbb{E}_x[v_{\theta,x} - C_v + C_v]^\top \mathbb{E}_x[w_{\theta,x}(t) - C_w + C_w] dt \quad (31)$$

$$= \int_0^T \mathbb{E}_x[v_{\theta,x}(t) - C_v]^\top \mathbb{E}_x[w_{\theta,x}(t) - C_w] dt \quad (32)$$

$$+ \int_0^T \mathbb{E}_x[v_{\theta,x}(t) - C_v]^\top \mathbb{E}_x[C_w] dt \quad (33)$$

$$+ \int_0^T \mathbb{E}_x[C_v]^\top \mathbb{E}_x[w_{\theta,x}(t) - C_w] + T \mathbb{E}_x[C_v]^\top \mathbb{E}_x[C_w] \quad (34)$$

Because C_w does not depend on t , we can factor it out of the integral

$$\int_0^T \mathbb{E}_x[v_{\theta,x}(t) - C_v]^\top \mathbb{E}_x[C_w] dt = \left(\int_0^T \mathbb{E}_x[v_{\theta,x}(t) - C_v] dt \right)^\top \mathbb{E}_x[C_w] \quad (35)$$

Because $v_{\theta,x}$ is integrable on $[0, T] \times \Omega$ Fubini's Theorem applies and the order of integration can be interchanged, yielding

$$\left(\int_0^T \mathbb{E}_x[v_{\theta,x}(t) - C_v] dt \right)^\top \mathbb{E}_x[C_w] = \left(\mathbb{E}_x \left[\int_0^T v_{\theta,x}(t) - C_v dt \right] \right)^\top \mathbb{E}_x[C_w] \quad (36)$$

$$= (\mathbb{E}_x[0])^\top \mathbb{E}_x[C_w] \quad (37)$$

$$= 0, \quad (38)$$

where we used $\int_0^T (v_{\theta,x}(t) - C_v) dt = 0$. A similar derivation yields

$$\int_0^T \mathbb{E}_x[w_{\theta,x}(t) - C_w]^\top \mathbb{E}_x[C_v] dt = 0 \quad (39)$$

Therefore, we have

$$\int_0^T \mathbb{E}_x[v_{\theta,x}(t)]^\top \mathbb{E}_x[w_{\theta,x}(t)] dt = \int_0^T \mathbb{E}_x[v_{\theta,x}(t) - C_v]^\top \mathbb{E}_x[w_{\theta,x}(t) - C_w] dt + T \mathbb{E}_x[C_v]^\top \mathbb{E}_x[C_w] \quad (40)$$

$$\int_0^T \mathbb{E}_x[v_{\theta,x}(t)]^\top \mathbb{E}_x[w_{\theta,x}(t)] dt = \int_0^T \mathbb{E}_x[v_{\theta,x}(t) - C_v]^\top \mathbb{E}_x[w_{\theta,x}(t) - C_w] dt + \frac{1}{T} E_1^\top E_2 \quad (41)$$

By Cauchy-Schwarz and Assumption 4.6, $\forall t$

$$\mathbb{E}_x[v_{\theta,x}(t) - C_v]^\top \mathbb{E}_x[w_{\theta,x}(t) - C_w] \leq \|\mathbb{E}_x[v_{\theta,x} - C_v]\| \|\mathbb{E}_x[w_{\theta,x} - C_w]\| \quad (42)$$

$$\leq (a_v + \delta_v \|\mathbb{E}_x[\nabla_\theta J_x]\|)(a_w + \delta_w \|\mathbb{E}_x[d_x^{JFB}]\|) \quad (43)$$

$$\leq \max(a_v + \delta_v \|\mathbb{E}_x[\nabla_\theta J_x]\|, a_w + \delta_w \|\mathbb{E}_x[d_x^{JFB}]\|)^2 \quad (44)$$

$$\leq \delta_\theta^2 - \frac{\epsilon_v}{T^2} \|\mathbb{E}_x[\nabla_\theta J_x]\|^2 \quad (45)$$

Applying (45) and algebraically rearranging (41) yields

$$\int_0^T \mathbb{E}_x[v_{\theta,x}(t)]^\top \mathbb{E}_x[w_{\theta,x}(t)] dt \leq \int_0^T \delta_\theta^2 - \frac{\epsilon_v}{T^2} \|\nabla_\theta J_x\|^2 dt + \frac{1}{T} E_1^\top E_2 \quad (46)$$

$$E_1^\top E_2 \geq T \int_0^T \mathbb{E}_x[v_{\theta,x}(t)]^\top \mathbb{E}_x[w_{\theta,x}(t)] - \left(\delta_\theta^2 - \frac{\epsilon_v}{T^2} \|\mathbb{E}_x[\nabla_\theta J_x]\|^2 \right) dt \quad (47)$$

Thus, by the result of Lemma 4.7

$$E_1^\top E_2 \geq T \int_0^T \delta_\theta^2 - \left(\delta_\theta^2 - \frac{\epsilon_v}{T^2} \|\mathbb{E}_x[\nabla_\theta J_x]\|^2 \right) dt \quad (48)$$

$$E_1^\top E_2 \geq T \int_0^T \frac{\epsilon_v}{T^2} \|\mathbb{E}_x[\nabla_\theta J_x]\|^2 dt \quad (49)$$

$$E_1^\top E_2 \geq T \left(\frac{\epsilon_v}{T} \|\mathbb{E}_x[\nabla_\theta J_x]\|^2 \right) \quad (50)$$

$$E_1^\top E_2 \geq \epsilon_v \|\mathbb{E}_x[\nabla_\theta J_x]\|^2 \quad (51)$$

□

A.3. Proof of Lemma 4.9

Lemma 4.9: Under Assumptions 4.1 - 4.6, JFB-based SGD iterations (22) satisfy

$$\begin{aligned} \mathbb{E}_{\xi_j} [\mathbb{E}_x [J_x(\theta_{j+1})]] - \mathbb{E}_x [J_x(\theta_j)] &\leq \\ &- \alpha_j \epsilon_v \|\mathbb{E}_x [\nabla_\theta J_x(\theta_j)]\|^2 + \frac{\alpha_j^2 L_J B_{\max}^2 T^2}{2\beta} \end{aligned}$$

Proof. Let $F(\theta_j) = \mathbb{E}_x [J_x(\theta_j)]$ and $\nabla_\theta F(\theta_j) = \nabla_\theta \mathbb{E}_x [J_x(\theta_j)] = \mathbb{E}_x [\nabla_\theta J(\theta_j)]$ since $\mathbb{E}_x [\cdot]$ is an integral with respect to x , not θ . Taking the 2nd order Taylor expansion of F with respect to θ centered at θ_j , using the fact that J , and therefore F , is L_J -Lipschitz

$$F(\theta_{j+1}) \leq F(\theta_j) + \nabla_\theta F(\theta_j)^\top (\theta_{j+1} - \theta_j) + \frac{1}{2} L_J \|\theta_{j+1} - \theta_j\|^2$$

Using (22), we have

$$F(\theta_{j+1}) - F(\theta_j) \leq -\alpha_j \nabla_\theta F(\theta_j)^\top d_{\xi_j}^{JFB}(\theta_j) + \frac{\alpha_j}{2} L_J \|d_{\xi_j}^{JFB}(\theta_j)\|^2.$$

Taking the conditional expectation with respect to ξ_j on both sides of (A.3), we get

$$\begin{aligned} \mathbb{E}_{\xi_j} [F(\theta_{j+1})] - F(\theta_j) &\leq \mathbb{E}_{\xi_j} [-\alpha_j \nabla_\theta F(\theta_j)^\top d_{\xi_j}^{JFB}(\theta_j)] + \mathbb{E}_{\xi_j} [\frac{1}{2} \alpha_j^2 L_J \|d_{\xi_j}^{JFB}(\theta_j)\|^2] \\ &= -\alpha_j \nabla_\theta F(\theta_j)^\top \mathbb{E}_{\xi_j} [d_{\xi_j}^{JFB}(\theta_j)] + \mathbb{E}_{\xi_j} [\frac{1}{2} \alpha_j^2 L_J \|d_{\xi_j}^{JFB}(\theta_j)\|^2]. \end{aligned} \quad (52)$$

Note that, θ_j depends only on $\xi_{j-1}, \dots, \xi_1, \xi_0$ generated in previous iterates and $\mathbb{E}_{\xi_j} [F(\theta_j)] = F(\theta_j)$. By Cauchy-Schwarz inequality,

$$\left\| \int_0^T M_{\theta_j}^\top h_{\theta,x} dt \right\|^2 \leq \left(\int_0^T 1^2 dt \right) \left(\int_0^T \|M_{\theta_j}^\top h_{\theta,x}\|^2 dt \right) = T \int_0^T \|M_{\theta_j}^\top h_{\theta,x}\|^2 dt \leq T \int_0^T \|M_{\theta_j}^\top\|^2 \|h_{\theta,x}\|^2 dt.$$

Thus, by Assumptions 4.3- 4.4,

$$\mathbb{E}_{\xi_j} [\|d_{\xi_j}^{JFB}(\theta_j)\|^2] = \mathbb{E} \left[\left\| \frac{1}{B} \sum_{b=1}^B d_{x_b}^{JFB}(\theta_j) \right\|^2 \right] \leq \mathbb{E}_x [\|d_x^{JFB}(\theta_j)\|^2] \leq \frac{B_{\max}^2 T^2}{\beta}, \quad (53)$$

where we remind the reader that $d_{\xi_j}^{JFB}(\theta_j)$ may correspond to the JFB gradient computed on a minibatch of samples and $d_x^{JFB}(\theta_j)$ corresponds to the JFB gradient computed on a single sample.

Thus, by the result of Lemma 4.8, (52), (53), and the fact that $\mathbb{E}_{\xi_j} [d_{\xi_j}^{JFB}(\theta_j)] = \mathbb{E}_x [d_x^{JFB}(\theta_j)]$, it holds that

$$\mathbb{E}_{\xi_j} [\mathbb{E}_x [J_x(\theta_{j+1})]] - \mathbb{E}_x [J_x(\theta_j)] \leq -\alpha_j \epsilon_v \|\mathbb{E}_x [\nabla_\theta J_x(\theta_j)]\|^2 + \frac{\alpha_j^2 L_J B_{\max}^2 T^2}{2\beta} \quad (54)$$

It can be derived that the RHS of (54) is ≤ 0 when α_j satisfies $0 < \alpha_j \leq \frac{2\epsilon_v}{L_J(1-\gamma)^2}$. \square

A.4. Proof of Theorem 4.10

Theorem 4.10: Suppose the sequence of learning rates $\{\alpha_j\}_{j=0}^\infty$ is monotonically decreasing and satisfies $\sum_{j=0}^\infty \alpha_j = \infty$, $\sum_{j=0}^\infty \alpha_j^2 < \infty$, and $0 < \alpha_0 \leq \frac{2\epsilon_v}{L_J(1-\gamma)^2}$. Let $A_K = \sum_{j=0}^K \alpha_j$. Then, under Assumptions 4.1- 4.6, the JFB-based SGD iteration (22) satisfies

$$\lim_{K \rightarrow \infty} \mathbb{E} \left[\frac{1}{A_K} \sum_{j=0}^K \alpha_j \|\mathbb{E}_x [\nabla_\theta J_x(\theta_j)]\|^2 \right] = 0.$$

Proof. Taking the total expectation of (54), we have

$$\mathbb{E}[\mathbb{E}_x[J_x(\theta_{j+1})]] - \mathbb{E}[\mathbb{E}_x[J_x(\theta_j)]] \leq -\alpha_j \epsilon_v \mathbb{E}[\|\mathbb{E}_x[\nabla_\theta J_x(\theta_j)]\|^2] + \frac{\alpha_j^2 L_J B_{max}^2 T^2}{2\beta} \quad (55)$$

Setting $j = 0$ in (55), we have

$$\mathbb{E}[\mathbb{E}_x[J_x(\theta_1)]] \leq \mathbb{E}[\mathbb{E}_x[J_x(\theta_0)]] - \alpha_j \epsilon_v \mathbb{E}[\|\mathbb{E}_x[\nabla_\theta J_x(\theta_0)]\|^2] + \frac{\alpha_j^2 L_J B_{max}^2 T^2}{2\beta} \quad (56)$$

Setting $j = 1$ in (55) and applying (56)

$$\begin{aligned} \mathbb{E}[\mathbb{E}_x[J_x(\theta_2)]] &\leq \mathbb{E}[\mathbb{E}_x[J_x(\theta_1)]] - \alpha_j \epsilon_v \mathbb{E}[\|\mathbb{E}_x[\nabla_\theta J_x(\theta_1)]\|^2] + \frac{\alpha_j^2 L_J B_{max}^2 T^2}{2\beta} \\ \mathbb{E}[\mathbb{E}_x[J_x(\theta_2)]] &\leq \mathbb{E}[\mathbb{E}_x[J_x(\theta_0)]] - \epsilon_v \sum_{j=0}^1 \alpha_j \mathbb{E}[\|\mathbb{E}_x[\nabla_\theta J_x(\theta_j)]\|^2] + \frac{L_J B_{max}^2 T^2}{2\beta} \sum_{j=0}^1 \alpha_j^2 \\ \mathbb{E}[\mathbb{E}_x[J_x(\theta_2)]] - \mathbb{E}[\mathbb{E}_x[J_x(\theta_0)]] &\leq -\epsilon_v \sum_{j=0}^1 \alpha_j \mathbb{E}[\|\mathbb{E}_x[\nabla_\theta J_x(\theta_j)]\|^2] + \frac{L_J B_{max}^2 T^2}{2\beta} \sum_{j=0}^1 \alpha_j^2 \\ &\vdots \\ \mathbb{E}[\mathbb{E}_x[J_x(\theta_K)]] - \mathbb{E}[\mathbb{E}_x[J_x(\theta_0)]] &\leq -\epsilon_v \sum_{j=0}^{K-1} \alpha_j \mathbb{E}[\|\mathbb{E}_x[\nabla_\theta J_x(\theta_j)]\|^2] + \frac{L_J B_{max}^2 T^2}{2\beta} \sum_{j=0}^{K-1} \alpha_j^2 \end{aligned}$$

Since J_x is bounded from below by J_{inf} by Assumption 4.1, algebraically rearranging the last line above yields

$$\sum_{j=0}^{K-1} \alpha_j \mathbb{E}[\|\mathbb{E}_x[\nabla_\theta J_x(\theta_j)]\|^2] \leq \frac{\mathbb{E}[\mathbb{E}_x[J_x(\theta_0)]] - J_{inf}}{\epsilon_v} + \frac{L_J B_{max}^2 T^2}{2\beta \epsilon_v} \sum_{j=0}^{K-1} \alpha_j^2 \quad (57)$$

$$\frac{1}{A_K} \sum_{j=0}^{K-1} \alpha_j \mathbb{E}[\|\mathbb{E}_x[\nabla_\theta J_x(\theta_j)]\|^2] \leq \frac{\mathbb{E}[\mathbb{E}_x[J_x(\theta_0)]] - J_{inf}}{\epsilon_v A_K} + \frac{L_J B_{max}^2 T^2}{2\beta \epsilon_v A_K} \sum_{j=0}^{K-1} \alpha_j^2 \quad (58)$$

Using linearity of expectation, (58) becomes

$$\mathbb{E} \left[\frac{1}{A_K} \sum_{j=0}^{K-1} \alpha_j \|\mathbb{E}_x[\nabla_\theta J_x(\theta_j)]\|^2 \right] \leq \frac{\mathbb{E}[\mathbb{E}_x[J_x(\theta_0)]] - J_{inf}}{\epsilon_v A_K} + \frac{L_J B_{max}^2 T^2}{2\beta \epsilon_v A_K} \sum_{j=0}^{K-1} \alpha_j^2 \quad (59)$$

Thus, since $\lim_{K \rightarrow \infty} A_K = \infty$, we have

$$\begin{aligned} &\lim_{K \rightarrow \infty} \mathbb{E} \left[\frac{1}{A_K} \sum_{j=0}^{K-1} \alpha_j \|\mathbb{E}_x[\nabla_\theta J_x(\theta_j)]\|^2 \right] \\ &\leq \lim_{K \rightarrow \infty} \left[\frac{2\beta(\mathbb{E}[\mathbb{E}_x[J_x(\theta_0)]] - J_{inf}) + L_J B_{max}^2 T^2 L \sum_{j=0}^{K-1} \alpha_j^2}{2\beta \epsilon_v A_K} \right] \\ &= 0 \end{aligned}$$

□

A.5. Proof of Theorem 4.11

Theorem 4.11: Under the assumptions of Theorem 4.10, the JFB-based SGD iteration (22) satisfies

$$\liminf_{j \rightarrow \infty} \mathbb{E} \left[\|\mathbb{E}_x[\nabla_\theta J_x(\theta_j)]\|^2 \right] = 0.$$

Proof. Suppose, for contradiction that, for some $a > 0$

$$\liminf_{j \rightarrow \infty} \mathbb{E} \left[\|\mathbb{E}_x[\nabla_\theta J_x(\theta_j)]\|^2 \right] = a \quad (60)$$

Let $K \in \mathbb{N}$ and $A_K = \sum_{k=0}^K \alpha_k$. Then, using linearity of expectation

$$\mathbb{E} \left[\frac{1}{A_K} \sum_{j=0}^K \alpha_j \|\mathbb{E}_x[\nabla_\theta J_x(\theta_j)]\|^2 \right] = \frac{1}{A_K} \sum_{j=0}^K \mathbb{E} \left[\|\mathbb{E}_x[\nabla_\theta J_x(\theta_j)]\|^2 \right]$$

Taking the liminf as $K \rightarrow \infty$ on both sides of the above equation yields a contradiction, as the LHS converges to 0 but the RHS diverges. Hence, by contradiction the result follows. \square

A.6. Proof of Corollary 4.12

Corollary 4.12: Suppose the assumptions of Theorem 4.10 hold. For any $K \in \mathbb{N}$ let $j(K) \in \{0, 1, \dots, K\}$ represent a random index chosen with probabilities proportional to $\{\alpha_j\}_{j=0}^K$. Then, $\{\|\mathbb{E}_x[\nabla_\theta J_x(\theta_j)]\|\}_{j=0}^K \rightarrow 0$ as $K \rightarrow \infty$ in probability.

Proof. This proof is the same as that of Theorem 4.11 in (Bottou et al., 2018) but we will include it here to be complete. Let $\epsilon > 0$ and let $\mathbb{E}[\cdot]$ represent total expectation. By Markov's inequality and the law of total expectation, also known as the tower property,

$$P(\|\mathbb{E}_x[\nabla_\theta J_x(\theta_{j(K)})]\| \geq \epsilon) = P(\|\mathbb{E}_x[\nabla_\theta J_x(\theta_{j(K)})]\|^2 \geq \epsilon^2) \quad (61)$$

$$\leq \frac{1}{\epsilon^2} \mathbb{E}[\mathbb{E}_{j(K)}[\mathbb{E}_x[\nabla_\theta J_x(\theta_{j(K)})]]] \quad (62)$$

By the proof of Theorem 4.10 we have $\lim_{K \rightarrow \infty} \mathbb{E} \left[\sum_{j=0}^{K-1} \alpha_j \|\mathbb{E}_x[\nabla_\theta J_x(\theta_j)]\|^2 \right] < \infty$. Therefore, we must have $\lim_{j \rightarrow \infty} \mathbb{E}[\alpha_j \|\mathbb{E}_x[\nabla_\theta J_x(\theta_j)]\|^2] = 0$. Thus, by (62),

$$\lim_{K \rightarrow \infty} P(\|\mathbb{E}_x[\nabla_\theta J_x(\theta_{j(K)})]\| \geq \epsilon) \leq \lim_{K \rightarrow \infty} \frac{1}{\epsilon^2} \mathbb{E}[\mathbb{E}_{j(K)}[\mathbb{E}_x[\nabla_\theta J_x(\theta_{j(K)})]]] = 0 \quad (63)$$

Since the choice of $\epsilon > 0$ was arbitrary, this holds $\forall \epsilon > 0$, proving convergence in probability. \square

B. Problem Formulation for Optimal Consumption Savings

We consider a model for individual's consumption optimization. The wealth $x_t, t \in [0, T]$ of an individual follows

$$\frac{dx_t}{dt} = rx_t - \mathbf{1}^\top u_t,$$

with given initial condition x_0 . Here r is the risk-free rate, the individual choose a consumption strategy $u_t \in \mathbb{R}^m$ for m products, while tracking a habit level $h_t \in \mathbb{R}^m$, with given initial condition h_0 ,

$$\frac{dh(t)}{dt} = Au^{\circ\eta}(t) - Bh^{\circ\theta}(t),$$

where \circ denotes component-wise power. To simplify the setup, we take B to be diagonal with entries $B_i \geq 0$. An individual maximizes a CRRA-type discounted utility

$$\int_0^T e^{-\delta t} \frac{\sum_{i=1}^n (u_i(t) - h_i(t))^{1-\gamma}}{1-\gamma} dt + e^{-\delta T} \epsilon \frac{x_T^{1-\gamma}}{1-\gamma},$$

where $u_i(t) > h_i(t)$ for $i = 1, \dots, m$, and $\gamma \neq 1, \epsilon, \delta, \eta, \theta$ are positive constants. The consumption behavior exhibits habit formation, that is, the current utility depends on the consumption relative to an individual's habit level established from past consumption. Then, the Hamiltonian is

$$\mathcal{H}(t, x, h, u, p) = e^{-\delta t} \sum_{i=1}^m \frac{(u_i - h_i)^{1-\gamma}}{1-\gamma} + p_x(rx - \mathbf{1}^\top u) + p_h^\top (Au^{\circ\eta} - Bh^{\circ\theta}).$$

Let $\frac{\partial \mathcal{H}}{\partial u} = 0$, then $e^{-\delta t}(u - h)^{-\gamma} - p_x + \alpha \eta p_h u^{\eta-1} = 0$. This first-order condition does not have a closed-form solution in general.

C. Proof of Convergence of SGD with JFB as Stochastic Gradient to a Neighborhood of a Critical Point Under Weaker Assumptions

It is possible to prove convergence in expectation of JFB-based SGD using the iteration (22) to a neighborhood of a critical point of J under weaker assumptions than Theorem 4.10 depends on. This section was inspired by (Demidovich et al., 2024).

Assumption C.1. *Modify Assumption 4.5 to be $\exists 0 < \delta_{var} < \lambda_- - \gamma \lambda_+$ and $\epsilon_1 \geq 0$ such that $\forall z, u, \theta$*

$$\max(\text{Var}_x[v_{\theta,x}(t)], \text{Var}_x[w_{\theta,x}(t)])^2 \leq \epsilon_1 + \delta_{var} \|\mathbb{E}_x[M_\theta v_{\theta,x}]\|^2$$

Lemma C.2. *Under the Assumptions of 4.1- 4.4 and Assumption C.1, $\forall z, u, \theta$*

$$\langle \mathbb{E}_x[v_{\theta,x}(t)], \mathbb{E}_x[w_{\theta,x}(t)] \rangle \geq \delta_\theta^2 - \epsilon_1 \quad (64)$$

where δ_θ is defined in Assumption 4.6 and ϵ_1 is defined in Assumption C.1

Proof. Let $E_v = \mathbb{E}_x[v_{\theta,x}(t)]$, $E_w = \mathbb{E}_x[w_{\theta,x}(t)]$. With these assumptions and this notation, everything up to the line

$$\mathbb{E}_x[\langle v_{\theta,x}, w_{\theta,x} \rangle] \leq \max \left(\sqrt{\text{Var}_x[v_{\theta,x}]}, \sqrt{\text{Var}_x[w_{\theta,x}]} \right)^2 + \langle E_v, E_w \rangle \quad (65)$$

in the proof of Lemma 4.7 still holds. Applying Assumption C.1 to this equation gives

$$\mathbb{E}_x[\langle v_{\theta,x}, w_{\theta,x} \rangle] \leq \epsilon_1 + \delta_{var} \|\mathbb{E}_x[v_{\theta,x}]\|^2 + \langle E_v, E_w \rangle \quad (66)$$

$$\langle E_v, E_w \rangle \geq \mathbb{E}_x[\langle v_{\theta,x}, w_{\theta,x} \rangle] - \delta_{var} \|\mathbb{E}_x[v_{\theta,x}]\|^2 - \epsilon_1 \quad (67)$$

$$\langle E_v, E_w \rangle \geq (\lambda_- - \gamma \lambda_+) \|\mathbb{E}_x[M_\theta v_{\theta,x}]\|^2 - \delta_{var} \|\mathbb{E}_x[v_{\theta,x}]\|^2 - \epsilon_1 \quad (68)$$

$$\langle E_v, E_w \rangle \geq (\lambda_- - \gamma \lambda_+ - \delta_{var}) \|\mathbb{E}_x[M_\theta v_{\theta,x}]\|^2 - \epsilon_1 \quad (69)$$

$$\langle E_v, E_w \rangle \geq \delta_\theta^2 - \epsilon_1 \quad (70)$$

□

Lemma C.3. *Under Assumptions 4.1- 4.4, C.1, and 4.6, $\forall u, z, \theta$*

$$\mathbb{E}_x[\nabla_\theta J_x]^\top \mathbb{E}_x[d_x^{JFB}] \geq \epsilon_v \|\mathbb{E}_x[\nabla_\theta J_x]\|^2 - \epsilon'_1$$

where ϵ_v is given in Assumption 4.6 and $\epsilon'_1 = T^2 \epsilon_1$ with ϵ_1 is from Assumption C.1

Proof. Under these assumptions, everything in the proof of Lemma 4.8 up to and including the line

$$E_1^\top E_2 \geq T \int_0^T \mathbb{E}_x[v_{\theta,x}(t)]^\top \mathbb{E}_x[w_{\theta,x}(t)] - \left(\delta_\theta^2 - \frac{\epsilon_v}{T^2} \|\mathbb{E}_x[\nabla_\theta J_x]\|^2 \right) dt \quad (71)$$

still holds. Applying the result of Lemma C.2, we obtain

$$E_1^\top E_2 \geq T \int_0^T \delta_\theta^2 - \epsilon_1 - \left(\delta_\theta^2 - \frac{\epsilon_v}{T^2} \|\mathbb{E}_x[\nabla_\theta J_x]\|^2 \right) dt \quad (72)$$

$$E_1^\top E_2 \geq T \int_0^T \frac{\epsilon_v}{T^2} \|\mathbb{E}_x[\nabla_\theta J_x]\|^2 - \epsilon_1 dt \quad (73)$$

$$E_1^\top E_2 \geq \epsilon_v \|\mathbb{E}_x[\nabla_\theta J_x]\|^2 - T^2 \epsilon_1 = \epsilon_v \|\mathbb{E}_x[\nabla_\theta J_x]\|^2 - \epsilon'_1 \quad (74)$$

□

Theorem C.4. Under the assumptions of Lemma C.3, the JFB-based SGD iteration (22) with constant step size/learning rate $\alpha > 0$, will converge in (total) expectation to a neighborhood of the critical point

$$\lim_{K \rightarrow \infty} \mathbb{E} \left[\frac{1}{K} \sum_{j=1}^K \|\mathbb{E}_x[\nabla_\theta J_x]\|^2 \right] \leq \frac{\alpha^2 L_J B_{\max}^2 T^2}{2\beta} + \frac{\epsilon'_1}{\epsilon_v} \quad (75)$$

Proof. Under these assumptions, everything in the proof of Lemma 4.9 up to and including the line

$$\mathbb{E}_{\xi_j}[F(\theta_{j+1})] - F(\theta_j) \leq -\alpha_j \nabla_\theta F(\theta_j)^\top \mathbb{E}_{\xi_j}[d_{\xi_j}^{JFB}(\theta_j)] + \mathbb{E}_{\xi_j} \left[\frac{\alpha_j^2 L_J}{2} \|d_x^{JFB}(\theta_j)\|^2 \right] \quad (76)$$

still holds. Replacing F with $\mathbb{E}_x[J_x]$, $\mathbb{E}_{\xi_j}[d_{\xi_j}^{JFB}(\theta_j)]$ with $\mathbb{E}_x[d_x^{JFB}(\theta_j)]$ like in Lemma 4.9, and applying the result of Lemma C.3 and the upper bound $\mathbb{E}_{\xi_j}[\|d_{\xi_j}^{JFB}(\theta)\|^2] \leq \frac{B_{\max}^2 T^2}{\beta}$, we have

$$\mathbb{E}_{\xi_j}[\mathbb{E}_x[J_x(\theta_{j+1})]] - \mathbb{E}_x[J_x(\theta_j)] \leq -\alpha(\epsilon_v \|\mathbb{E}_x[\nabla_\theta J_x(\theta_j)]\|^2 - \epsilon'_1) + \frac{\alpha^2}{2} L_J \left(\frac{B_{\max}^2 T^2}{\beta} \right) \quad (77)$$

Taking total expectation of the above line, we have

$$\mathbb{E}[\mathbb{E}_x[J_x(\theta_{j+1})]] - \mathbb{E}[\mathbb{E}_x[J_x(\theta_j)]] \leq -\alpha(\epsilon_v \mathbb{E}[\|\mathbb{E}_x[\nabla_\theta J_x(\theta_j)]\|^2] - \epsilon'_1) + \frac{\alpha^2}{2} L_J \left(\frac{B_{\max}^2 T^2}{\beta} \right) \quad (78)$$

Setting $j = 0$ in (78), we have

$$\mathbb{E}[\mathbb{E}_x[J_x(\theta_1)]] - \mathbb{E}[\mathbb{E}_x[J_x(\theta_0)]] \leq -\alpha(\epsilon_v \mathbb{E}[\|\mathbb{E}_x[\nabla_\theta J_x(\theta_0)]\|^2] - \epsilon'_1) + \frac{\alpha^2}{2} L_J \left(\frac{B_{\max}^2 T^2}{\beta} \right) \quad (79)$$

$$\mathbb{E}[\mathbb{E}_x[J_x(\theta_1)]] \leq \mathbb{E}[\mathbb{E}_x[J_x(\theta_0)]] - \alpha(\epsilon_v \mathbb{E}[\|\mathbb{E}_x[\nabla_\theta J_x(\theta_0)]\|^2] - \epsilon'_1) + \frac{\alpha^2}{2} L_J \left(\frac{B_{\max}^2 T^2}{\beta} \right) \quad (80)$$

Setting $j = 1$ in (78) and applying (80) yields

$$\begin{aligned} \mathbb{E}[\mathbb{E}_x[J_x(\theta_2)]] - \mathbb{E}[\mathbb{E}_x[J_x(\theta_1)]] &\leq -\alpha(\epsilon_v \mathbb{E}[\|\mathbb{E}_x[\nabla_\theta J_x(\theta_1)]\|^2] - \epsilon'_1) + \frac{\alpha^2}{2} L_J \left(\frac{B_{\max}^2 T^2}{\beta} \right) \\ \mathbb{E}[\mathbb{E}_x[J_x(\theta_2)]] &\leq \mathbb{E}[\mathbb{E}_x[J_x(\theta_1)]] - \alpha(\epsilon_v \mathbb{E}[\|\mathbb{E}_x[\nabla_\theta J_x(\theta_1)]\|^2] - \epsilon'_1) + \frac{\alpha^2}{2} L_J \left(\frac{B_{\max}^2 T^2}{\beta} \right) \\ \mathbb{E}[\mathbb{E}_x[J_x(\theta_2)]] &\leq \mathbb{E}[\mathbb{E}_x[J_x(\theta_0)]] - \alpha(\epsilon_v \mathbb{E}[\|\mathbb{E}_x[\nabla_\theta J_x(\theta_0)]\|^2] - \epsilon'_1) + \frac{\alpha^2}{2} L_J \left(\frac{B_{\max}^2 T^2}{\beta} \right) - \\ &\quad \alpha(\epsilon_v \mathbb{E}[\|\mathbb{E}_x[\nabla_\theta J_x(\theta_1)]\|^2] - \epsilon'_1) + \frac{\alpha^2}{2} L_J \left(\frac{B_{\max}^2 T^2}{\beta} \right) \\ \mathbb{E}[\mathbb{E}_x[J_x(\theta_2)]] - \mathbb{E}[\mathbb{E}_x[J_x(\theta_0)]] &\leq -\alpha \sum_{j=0}^1 (\epsilon_v \mathbb{E}[\|\mathbb{E}_x[\nabla_\theta J_x(\theta_j)]\|^2] - \epsilon'_1) + (2) \frac{\alpha^2}{2} L_J \left(\frac{B_{\max}^2 T^2}{\beta} \right) \\ &\quad \vdots \\ \mathbb{E}[\mathbb{E}_x[J_x(\theta_K)]] - \mathbb{E}[\mathbb{E}_x[J_x(\theta_0)]] &\leq -\alpha \sum_{j=0}^{K-1} (\epsilon_v \mathbb{E}[\|\mathbb{E}_x[\nabla_\theta J_x(\theta_j)]\|^2] - \epsilon'_1) + K \left(\frac{\alpha^2 L_J B_{\max}^2 T}{2\beta} \right) \end{aligned}$$

Because $J_x(\theta)$ is bounded from below by J_{\inf} (restrict domain if necessary), the last line above becomes, using linearity of expectation,

$$\begin{aligned} \alpha \epsilon_v \mathbb{E} \left[\sum_{j=0}^{K-1} \|\mathbb{E}_x[\nabla_\theta J_x]\|^2 \right] &\leq \mathbb{E}[\mathbb{E}_x[\nabla_\theta J_x(\theta_0)]] - J_{\inf} + \alpha K \left(\frac{\alpha B_{\max}^2 T L_J}{2\beta} + \epsilon'_1 \right) \\ \mathbb{E} \left[\frac{1}{K} \sum_{j=0}^{K-1} \|\mathbb{E}_x[\nabla_\theta J_x]\|^2 \right] &\leq \frac{\mathbb{E}[\mathbb{E}_x[\nabla_\theta J_x(\theta_0)]] - J_{\inf}}{K \alpha \epsilon_v} + \left(\frac{\alpha B_{\max}^2 T L_J}{2\beta \epsilon_v} + \frac{\epsilon'_1}{\epsilon_v} \right) \end{aligned}$$

Thus,

$$\lim_{K \rightarrow \infty} \mathbb{E} \left[\frac{1}{K} \sum_{j=0}^K \|\mathbb{E}_x[\nabla_{\theta} J_x(\theta_j)]\|^2 \right] \leq \lim_{K \rightarrow \infty} \left[\frac{\mathbb{E}[\mathbb{E}_x[\nabla_{\theta} J_x(\theta_0)]] - J_{inf}}{K \alpha \epsilon_v} + \frac{\alpha B_{max}^2 T L_J}{2 \beta \epsilon_v} + \frac{\epsilon'_1}{\epsilon_v} \right] \quad (81)$$

$$= \frac{\alpha L_J B_{max}^2 T^2}{2 \beta \epsilon_v} + \frac{\epsilon'_1}{\epsilon_v} \quad (82)$$

□

It can be seen from the result of Theorem C.4 that as $\alpha \rightarrow 0$, $\frac{\alpha L_J B_{max}^2 T^2}{2 \beta \epsilon_v} \rightarrow 0$, leaving only $\frac{\epsilon'_1}{\epsilon_v}$. Thus, even if a decreasing step size is used, like in Theorem 4.10, it is impossible to achieve

$$\liminf_{j \rightarrow \infty} \mathbb{E} [\|\mathbb{E}_x[\nabla_{\theta} J_x(\theta_j)]\|^2] = 0 \quad (83)$$

under Assumption C.1. The JFB-based SGD iteration (22) will only be able to, at best, in expectation, get to a neighborhood of radius $\frac{\epsilon'_1}{\epsilon_v}$ of a critical point of J .